Structural Engineering and Mechanics, Vol. 23, No. 1 (2006) 1-13
DOI: http://dx.doi.org/10.12989/sem.2006.23.1.001

A generalized algorithm for the study of bilinear vibrations of cracked structures

Tzuo-Liang Luo† and James Shih-Shyn Wu‡

Institute of Mechanical Engineering, National Chung-Hsing University, 250, Kuo-Kuang Rd., Taichung, Taiwan 402, ROC

Jui-Pin Hung‡†

Institute of Precision Machinery and Manufacturing Technology, National Chin-Yi Institute of Technology, 35, Lane. 215, Sec. 1, Chung-Shan Rd., Taiping, Taichung, Taiwan 411, ROC

(Received February 24, 2005, Accepted January 23, 2006)

Abstract. Structural cracks may cause variations in structural stiffness and thus produce bilinear vibrations to structures. This study examines the dynamic behavior of structures with breathing cracks. A generalized algorithm based on the finite element method and bilinear theory was developed to study the influence of a breathing crack on the vibration characteristic. All the formulae derived in the time domain were applied to estimate the period of the overall bilinear motion cycle, and the contact effect was considered in the calculations by introducing the penetration of the crack surface. Changes in the dynamic characteristics of cracked structures are investigated by assessing the variation of natural frequencies under different crack status in either the open or closed modes. Results in estimation with vibrational behavior variation are significant compared with the experimental results available in the literature as well as other numerical calculations.

Keywords: breathing crack; cracked structure; finite element analysis.

1. Introduction

Structural components frequently fail when subjected to repeat or impact loads. Such failure generally occurs on crack sites owing to inappropriate manufacturing, operation or fatigue. To avoid irreparable damage, techniques for on-line crack monitoring and location are necessary. Since the contact or impact on the crack tip creates discontinuities near the crack sites, non-linear vibration behavior may be considered.

To avert complex non-linearity in essence, numerous investigations of cracked structures have been performed by assuming that the crack surface is persistently in the open state. However, this hypothesis frequently conflicts with reality. Intermittent contact between the loosely connected

† PhD Candidate
‡ PhD, Professor, Corresponding author, E-mail: sswu@dragon.nchu.edu.tw
‡† PhD, Associate Professor

components of a mechanical system frequently occurs during surgery. One typical example is the roll-bearings with radial clearance, which display a non-continuous rolling motion in grooves thus may cause changes in the dynamic characteristics of structures, including vibrating amplitudes and natural frequencies. On the other hand, small cracks or defects in mechanical components generate discontinuities in geometry, causing variations in structural stiffness and making dynamic characteristics difficult to predict. Since the measurement of the change of natural frequency for damaged structures can provide information relating crack appearance or crack depth (Chondros *et al.* 1980, Liew *et al.* 1998), vibration monitoring has been utilized to examine cracks and flaws in structures during the last three decades (Dimarogonas *et al.* 1996).

To ensure design and application safety, it is necessary to consider the dynamic behaviors of structures with embedded micro-cracks. Consequently, several different approaches based on either analytical or numerical analyses have been adopted for identifying such characteristics in cracked beam structures during the past decade. In certain cases, both sides of the crack were assumed to constantly be in an open state (Hjelmstad *et al.* 1996, Krawczuk *et al.* 1993, Kikidis 1992, Murphy *et al.* 2000). Some investigations used the Rayleigh principle and Wavelet theory to estimate the change in natural frequencies and dynamic sensitivity to surface crack (Chondros *et al.* 1989, Liew *et al.* 1998). However, the crack front, remaining in an open or closed state during vibration, is influenced by the degree of amplitude or by mutual collision of crack front surface. A cracked structure with a breathing crack thus may exhibit non-linear characteristics with different extents of motion (Kisa *et al.* 2000, Nandi *et al.* 2002, Chondros *et al.* 2001), where such extents depend on the vibrational amplitude and its mode shape. This increases the vibrational behavior complexity of cracked structures with a breathing crack. Therefore, to solve breathing crack problems in beams, numerous investigations used an elastic rotational spring to represent the discontinuous stiffness or local flexibility on the cracked section (Narkis 1994, Lee *et al.* 1994, Yokoyama *et al.* 1998, Chen *et al.* 1997, Lin *et al.* 2004, Fernandez *et al.* 2002). The spring constant was obtained based on Fracture Mechanics (Chen *et al.* 1997, Kisa 2004).

Most studies adopting the analytical approach extended the one-dimensional Euler-Bernoulli beam to simulate a uniform cracked beam with a single-edge crack or multiple cracks (Bovsunovsky *et al.* 2000, Chondros *et al.* 1998, Shen *et al.* 1990). The implicit solutions for natural frequency thus could be obtained. However, such analytical methods generally cannot directly provide explicit results for cracked beams with different boundary conditions, or with different crack types. Some other approaches using the finite element method were demonstrated to be efficient in predicting the dynamic behaviors of complicated crack structures (Gounaris *et al.* 1988, Qian *et al.* 1990, Khiem 2001, 2002). These studies introduce construction of the stiffness matrix of finite element beam models with the cracked segment.

To consider the variation in local stiffness owing to cracking, Gounaris (1988) and Khiem (2001), respectively, proposed crack compliance matrices for conjugating with other intact beam sections in the finite element models. Based on this idea, Khiem (2002) designed a dynamic stiffness matrix method for simulating a multiple cracked beam. Beyond that discussed above for the analytical approach where cracks were simulated with a rotational spring element, Chondros (1998) introduced the continuous cracked beam vibration theory, in which the stress field induced by the crack or flaw decays with distance from that crack or flaw. However, as discussed in Carson (1974) and Gudmundson (1983), a breathing crack exhibits different structural stiffness before and following the crack surfaces contact during vibration, which may change the motion behaviors in the bilinear vibrational modes. Thus, using the single equivalent elastic spring element it is really difficult to

effectively describe the bilinear vibration characteristics and the contact effect on the dynamic behaviors. Generally, the mutual contact effect of crack sites during the closing period may cause the increment of stiffness and constraint on the cracked section. For accurately forecasting crack structure dynamic behavior, the contact effect must be considered.

This study introduces a generalized finite element procedure based on the bilinear vibration theory with the contact effect of crack sites. The dynamic behaviors of cracked structures are also demonstrated. The following includes all formulae derived in the time domain that include the motion constraints in vibration.

2. Constrained motion theory and formulation

In practice, the displacement constraints on the crack sides affect the vibrational behavior of a cracked structure. Any finite element nodes on both sides of the crack surface must be controlled when the crack sides close or open during vibration. Therefore, the bilinear vibration behavior of a cracked structure must be simulated in the form of a three-dimensional system with proper motion constraints. The following derives the bilinear natural frequency of a vibrating system with proper displacement constraints.

2.1 Period of bilinear motion

In Fig. 1, a mass m_i vibrates freely with amplitude x_{0i} on one side but with an elastic boundary placed at x_{ci} on the opposite side. When the motion is constrained at x_{ci}, the mass may penetrate into the boundary with a depth of $(x_{pi}-x_{ci})$ following contact with the elastic boundary. At this point, bilinear motion will occur and the relationship of x_i and $\dot{x}_i$ will exhibit the asymmetrical motion depicted during the phase plane, as shown in Fig. 2, which differs markedly from a full ellipse type of free vibration. The completion of one cycle thus comprises two parts: free motion period and constrained motion period. This can be estimated using the following integrating form.

$$T_i = 2\oint_{\Gamma_i} dt = 2(T^- + T^+) \tag{1}$$

where Γ_i represents the motion trajectory in the phase plane refer to Fig. 2. Moreover, T^- denotes the period of free motion from $-x_{0i}$ to x_{ci} and T^+ represents the period of constrained motion from x_{ci} to x_{pi}. Finally, $T^- = \oint_{\Gamma_{i-}} dt = \int_{x_{ci}}^{-x_{0i}} (1/\dot{x}^-)dx^-$ and $T^+ = \oint_{\Gamma_{i+}} dt = \int_{x_{pi}}^{x_{ci}} (1/\dot{x}^+)dx^+$

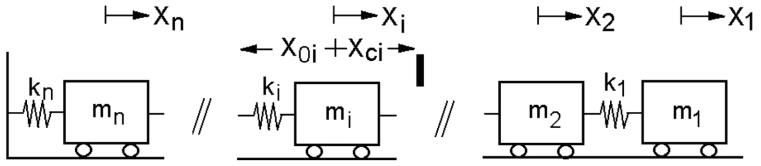

Fig. 1 Schematic of a multi-degree-of-freedom system. A constrained boundary is located at x_{ci} to restrict the motion of ith mass.

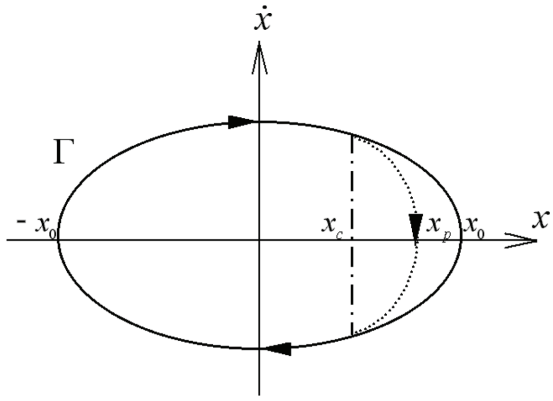

$-x_0 \sim x_c$: Displacement interval for breathing crack with rigid boundary

$-x_0 \sim x_p$: Displacement interval for breathing crack with elastic boundary

$-x_0 \sim x_0$: Displacement interval for opening crack mode in free vibration

$x_c \sim x_p$:Penetration distance

Fig. 2 A bilinear motion plotted on the phase plane as a comparison of motion loci for opening crack mode and breathing crack mode

For a multi-degree-of-freedom system, equations of motion can be expressed in dummy index form

$$m_{ij}\ddot{x}_j + k_{ij}x_j = 0 \tag{2}$$

The well-known sinusoidal solution of Eq. (2) for the ith mode equals

$$x_j = x_{oj}\sin\omega_i t \tag{3}$$

where j denotes the cyclic index for the nodal degrees of freedom.

Now, replacing terms by $\dot{x}_j = dx_j/dt$ and $\ddot{x}_j = d\dot{x}_j/dt$ in Eq. (2) yields

$$m_{ij}\frac{d\dot{x}_j}{dx_j}\frac{dx_j}{dt} + k_{ij}x_j = 0 \tag{4}$$

An alternative form of Eq. (2) can be written as

$$m_{ij}\frac{d\dot{x}_j}{dx_j} + \frac{k_{ij}x_j}{\dot{x}_j} = 0 \tag{5}$$

Eq. (4) can be integrated to yield

$$\int_0^{\dot{x}_j} m_{ij}\dot{x}_j d\dot{x}_j = \int_{-x_{0j}}^{x_j} -k_{ij}x_j dx_j = \frac{1}{2}m_{ij}\dot{x}_j^2 = \frac{1}{2}k_{ij}(x_{0j}^2 - x_j^2) \tag{6}$$

Eq. (6) is rewritten into the matrix form as

$$\frac{1}{2}[m]\{\dot{x}^2\} = \frac{1}{2}[k](\{x_0^2\} - \{x^2\}) \tag{7}$$

or

$$\{\dot{x}^2\} = [\hat{k}](\{x_0^2\} - \{x^2\}) \tag{8}$$

where $[\hat{k}] = [m]^{-1}[k]$.

The velocity vector $\{\dot{x}^2\}$ in Eq. (8) can be further expressed as

$$\dot{x}_i = [\hat{k}_{ij}(x_{0j}^2 - x_j^2)]^{\frac{1}{2}} = \hat{k}_{ij}^{\frac{1}{2}}\sqrt{(x_{0j}^2 - x_j^2)} = A_{ij}\sqrt{(x_{0j}^2 - x_j^2)} \tag{9}$$

and

$$\frac{1}{\dot{x}_i} = (A_{ij}\sqrt{(x_{0j}^2 - x_j^2)})^{-1} = \left(A_{ij}^{-1}\frac{1}{\sqrt{(x_{0j}^2 - x_j^2)}}\right) = \left(B_{ij}\frac{1}{\sqrt{(x_{0j}^2 - x_j^2)}}\right) \tag{10}$$

where $[A] = [[m]^{-1}[k]]^{\frac{1}{2}}$

2.1.1 Period of free motion

Using $dt = (1/\dot{x}_i)dx_i$ and substituting Eq. (10) into Eq. (1), the half period for free motion T^- can be obtained by integration with respect to time as

$$T_i^- = 2B_{ij}\int_{x_{ci}}^{-x_{0i}} \frac{dx_i}{\sqrt{(x_{0j}^2 - x_j^2)}} = 2B_{ij}\int_{x_{cj}}^{-x_{0j}} \frac{1}{\sqrt{(x_{0j}^2 - x_j^2)}}\frac{\partial x_i}{\partial x_j}dx_j \tag{11}$$

where $[B] = ([m]^{-1}[k])^{-\frac{1}{2}}$ in the matrix form and $B_{ij} = (m_{il}^{-1}k_{lj})^{-\frac{1}{2}}$ in the index form.
Clearly the derivation.

$$\frac{\partial x_i}{\partial x_j} = \frac{dx_i}{dt}\frac{dt}{dx_j} = \frac{\dot{x}_i}{\dot{x}_j} = \frac{d(x_{0i}\sin\omega_i t)/dt}{d(x_{0j}\sin\omega_i t)/dt} = \frac{x_{0i}}{x_{0j}}$$

Results in Eq. (13) having the following form

$$T_i^- = 2B_{ij}\int_{x_{cj}}^{-x_{0j}} \frac{1}{\sqrt{(x_{0j}^2 - x_j^2)}}\frac{x_{0i}}{x_{0j}}dx_j \tag{12}$$

Then, integration yields

$$T_i^- = 2B_{ij}\frac{x_{0i}}{x_{0j}}\left[\frac{\pi}{2} - \sin^{-1}\left(-\frac{x_{cj}}{x_{0j}}\right)\right] \tag{13}$$

Finally, the half period of free motion can be represented in matrix form as

$$T_i^- = 2x_{0i}\langle B_{i1}\ \ B_{i2}\ \ \ldots\ \ \ldots\ \ B_{in}\rangle\begin{Bmatrix} \frac{1}{x_{01}}\left[\frac{\pi}{2} - \sin^{-1}\frac{x_{c1}}{x_{01}}\right] \\ \frac{1}{x_{02}}\left[\frac{\pi}{2} - \sin^{-1}\frac{x_{c2}}{x_{02}}\right] \\ \vdots \\ \vdots \\ \frac{1}{x_{0n}}\left[\frac{\pi}{2} - \sin^{-1}\frac{x_{cn}}{x_{0n}}\right] \end{Bmatrix} \tag{14}$$

or, in an alternative form

$$\{T^{-}\}_{n\times 1} = 2[\hat{x}_0][B]\{x_c^0\} \tag{15}$$

Where

$$[\hat{x}_0] = \begin{bmatrix} x_{01} & 0 & \cdots & 0 \\ 0 & x_{02} & \cdots & 0 \\ \vdots & \vdots & \ddots & \vdots \\ 0 & 0 & \cdots & x_{0n} \end{bmatrix}_{n\times n} \quad \text{and} \quad \{x_c^0\} = \begin{Bmatrix} \frac{1}{x_{01}}\left[\frac{\pi}{2} - \sin^{-1}\left(\frac{-x_{c1}}{x_{01}}\right)\right] \\ \frac{1}{x_{02}}\left[\frac{\pi}{2} - \sin^{-1}\left(\frac{-x_{c2}}{x_{02}}\right)\right] \\ \vdots \\ \frac{1}{x_{0n}}\left[\frac{\pi}{2} - \sin^{-1}\left(\frac{-x_{cn}}{x_{0n}}\right)\right] \end{Bmatrix} \tag{16}$$

2.1.2 Period of constrained motion

In the constrained motion, if the mass oscillates with sufficient amplitude, it will have a significant depth of contact with the elastic boundary. Generally, the depth of penetration depends on the contact stiffness of the interface between the two contact bodies, and can be described using the following term C, as indicated by Butcher (1999) and Todoo (1996), respectively,

$$C = (x_{0i}/\alpha)\sqrt{1 - (x_{0i}^2/x_{0j}^2)(1 - 1/\alpha^2)}, \quad \alpha = \sqrt{1 + (x_{0j}/x_{cj})} \tag{17}$$

The period of constrained motion from x_{ci} to x_{pi} can thus be obtained by integrating T^{+} in Eq. (9) with $x_{pi} = x_{ci} + C$, that is

$$T^{+} = 2B_{ij}\frac{x_{0i}}{x_{0j}}\frac{1}{\alpha}\left[\frac{\pi}{2} - \sin^{-1}\left(-\frac{x_{cj}}{x_{0j}}\sqrt{1 - \frac{x_{cj}^2}{x_{0j}^2}\left(1 - \frac{1}{\alpha^2}\right)}\right)\right] \tag{18}$$

Finally, the total period of the bilinear motion can be obtained by adding the partial periods of each motion of the two regions:

$$T_i = 2B_{ij}\frac{x_{0i}}{x_{0j}}\left[\frac{\pi}{2} - \sin^{-1}\left(-\frac{x_{cj}}{x_{0j}}\right) + \frac{1}{\alpha}\left(\frac{\pi}{2} - \sin^{-1}\left(-\frac{x_{cj}}{x_{0j}}\sqrt{1 - \frac{x_{cj}^2}{x_{0j}^2}\left(1 - \frac{1}{\alpha^2}\right)}\right)\right)\right] \tag{19}$$

The bilinear natural frequency is represented by $\Omega_i = \frac{2\pi}{T_i}$.

3. Demonstrations

This study investigates two cases to determine the significance of the current method. Case 1 discusses a single-edge crack at the mid-span and case 2 discusses a single-edge crack at various locations. Owing to the presence of the crack, there is a $\sqrt{1/r}$ singularity in the stress field at crack tip (Chatti *et al.* 1997). Generally, quarter point (singular) elements are used to model the singular

behavior in the stress field. However, this analysis expects global changes in the structural stiffness rather than local variation in the stress field at the crack site. Additionally, the regular element was demonstrated to yield similar findings to the model meshed with singular element near crack site (Chatti *et al.* 1997). Therefore, regular hexahedron brick elements are adopted for model creation and further calculation.

3.1 Case 1: Single-edge crack at mid-span

To illustrate the proposed method, a cracked alumina beam used in experiment (Chondros *et al.* 2001) was adopted as a comparative example. The beam has a rectangular cross-section (width w = 7 mm and height h = 23 mm) and length 235 mm. The material properties are: Young's modulus

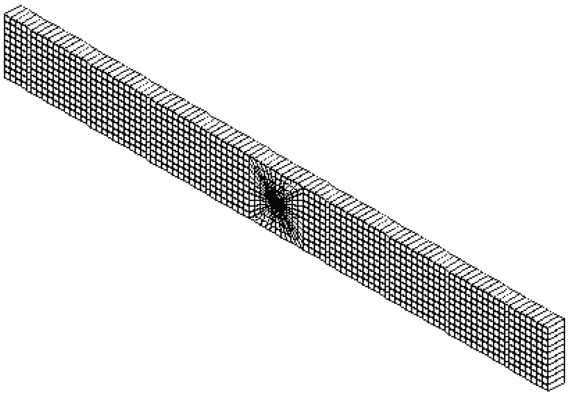

Fig. 3 The finite element model of a cracked beam with refined mesh at crack site

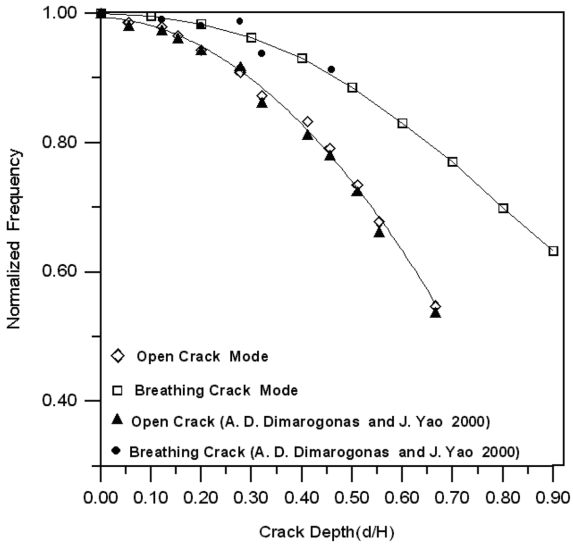

Fig. 4 Variation of the first normalized vibration frequency as a function of crack depth, compared with the results obtained in Chondros *et al.* (2001)

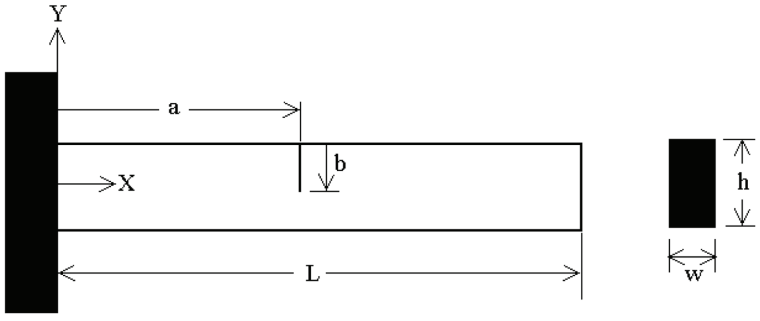

Fig. 5 Schematic of the cantilever cracked beam with a crack of depth b positioned at a

E = 72 GPa, density ρ = 2,800 kg/m^3 and Poisson's ratio ν = 0.3. For numerical analysis, a finite element model of the cracked beam is created and illustrated in Fig. 3, and a sharp notch perpendicular to the longitudinal axis is introduced at the mid span of the beam.

Fig. 4 shows the calculated results of the normalized natural frequencies versus the normalized crack depth of the cracked beam. Comparative experimental results obtained by Chondros *et al.* (2001) are also shown in Fig. 4 Clearly a crack with a large depth leads to a significant decrease in vibration frequency owing to the decrease of beam stiffness at the crack site. The current method also demonstrates that the vibrational frequency for the beam with a breathing crack exceeds that with an open crack. Notably, this cracked beam has a first bending vibration mode similar to that excited in the experiment by Chondros *et al.* (2001).

3.2 Case 2: Single-edge crack at various positions

The above-developed method was also applied to examine the effect of crack parameters (crack depth and crack position) on the dynamic behavior of a cantilever beam, as illustrated in Fig. 5. For validation, the beam shares the same geometry, material properties and boundary condition as the beam considered in the reference (Chatti *et al.* 1997). The steel beam has length L = 10 m and cross section area A = 1 m^2 with the following material properties: Young's modulus E = 210 GPa, density ρ = 7,850 kg/m^3 and Poisson's ratio ν = 0.3. This simulation assumes the crack positions of 0.2L, 0.5L, and 0.7L in FE cracked beam model and considers the first three natural modes.

Tables 1 and 2 show the predicted natural frequency of the cracked beam with various crack depths at different positions. Fig. 6 displays the variations of the first natural frequency expressed as

Table 1 Comparison of the fundamental natural frequency of a cracked beam with various crack depth and position

	Fundamental natural frequency (Hz)		
Crack depth ratio	Crack position (20 mm)	Crack position (50 mm)	Crack position (70 mm)
0.1	.81893	.82355	.82465
0.5	.63206	.76684	.82469
0.9	.18159	.27027	.75707

* Natural frequency of intact beam = .82494 Hz

Table 2 Comparison of the second natural frequency of a cracked beam with various crack depth and position

	Second natural frequency (Hz)		
Crack depth ratio	Crack position (20 mm)	Crack position (50 mm)	Crack position (7 0mm)
0.1	4.8782	4.5672	4.9484
0.5	4.7991	3.9380	4.9193
0.9	4.1694	3.1061	4.8310

* Natural frequency of intact beam = 4.9532 Hz

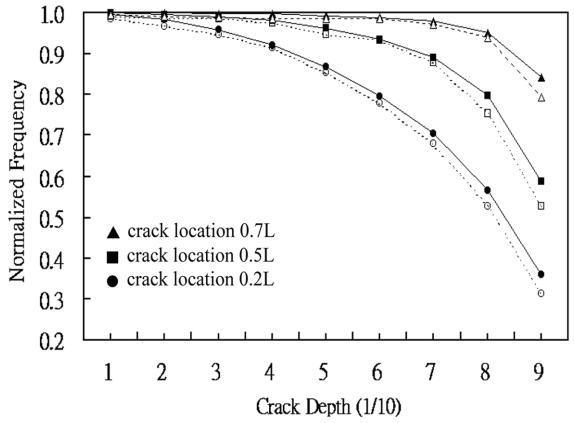

Fig. 6 Variations of first natural frequency as a function of the crack depth at different crack positions. Solid line: current FEM simulation results, dotted line: by bilinear method in Chatti *et al.* (1997)

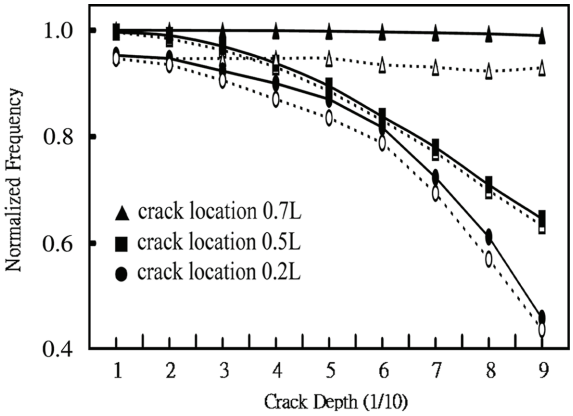

Fig. 7 Variations of second natural frequency as a function of the crack depth at different crack positions. Solid line: current FEM simulation results, dotted line: by bilinear method in Chatti *et al.* (1997)

a function of the crack depth for several crack positions. As expected, the vibration frequency decreases with crack depth, but the degree of influence depends on the crack position initiating in the beam. Furthermore, the major stiffness is dominated by the clamped part of the cantilever beam; as a consequence, a crack initiated near the fixed end of the beam yields a substantial decrease in frequency compared to free end.

Fig. 6 shows the results obtained by Chatti *et al.* (1997), which demonstrate good agreement in predicting frequency variation compared with the current results. A slight difference is also observable and is ascribed to the fact that Chatti *et al.* (1997) did not consider the variation of contact stiffness owing to the mutual interference of the crack interface during the crack closing period. Chatti *et al.* (1997) was based on the bilinear theory, in which two crack configurations (crack open and crack closed) were assumed in calculating the vibration frequency. In the constrained configuration, the fully closed crack was dealt with assuming a compatibility condition of displacement at the crack interface. This assumption may lead to the underestimation of beam stiffness across the crack site, and thus reduce the vibration frequency corresponding to the constrained motion, which is also referred to as the frequency of the closed crack in a bilinear system, as indicated by Gounaris *et al.* (1988). In fact, the crack surfaces of a breathing crack have restricted motion owing to interface contact during the closing period, but allowing mutual penetration at the interface. The motion path for the crack closing period thus is shortened by the constraint from the mutual interference at the crack interface. As a consequence, the time period of the constrained motion phase dominates the variation of the natural frequency of the cracked structures. Fig. 7 shows a similar comparison for the second vibration mode, which describes the results forecast using the current method and those obtained in Chatti *et al.* (1997). The figure clearly demonstrates good consistency in predicting the variation of the second natural frequency.

Referring once again to Tables 1 and 2, for a crack located at the midpoint the natural frequency reduces by approximately 7% for first mode and 20% for the second mode when the crack grows to half of the beam height. This implies that for a given crack location the reduction in natural

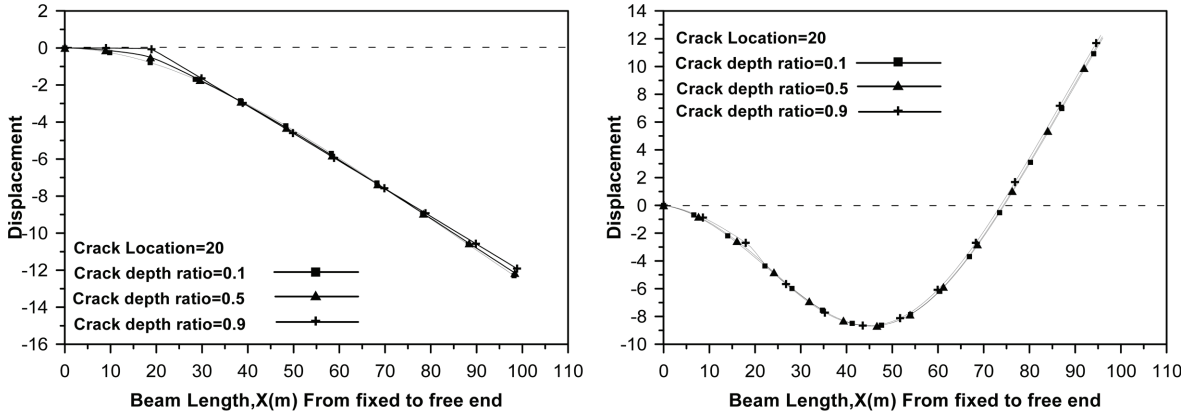

Fig. 8 Comparison of mode shape of cracked beam with a single-edge of different crack depth, crack positioned at 20 mm (a) first mode (b) second mode

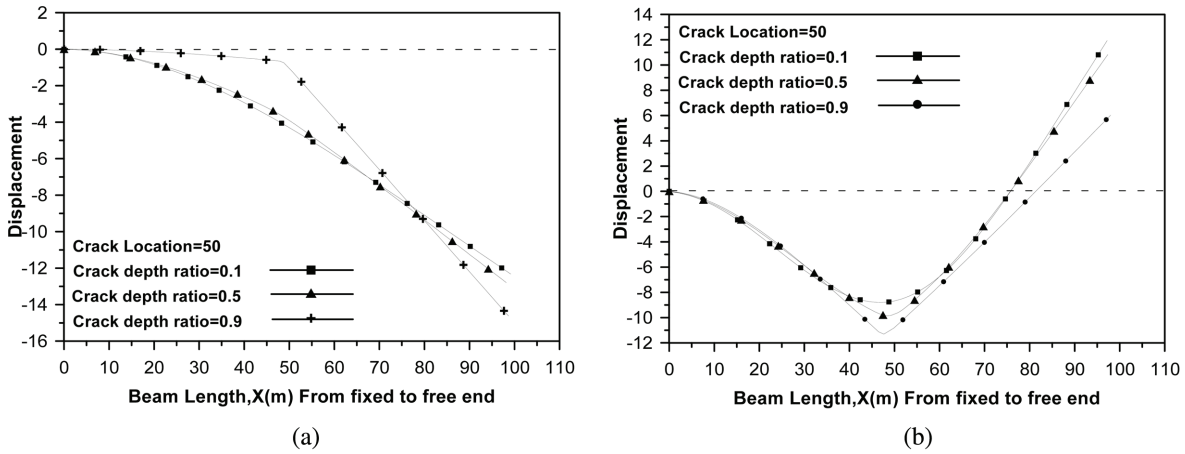

Fig. 9 Comparison of mode shape of cracked beam with a single-edge of different crack depth, crack positioned at 50 mm (a) first mode (b) second mode

frequencies increases with crack depth. The effect of the crack depth on the vibration behavior can be further observed from the mode shapes shown in Figs. 8 and 9, in which the crack was located at distances of 20 mm and 50 mm from the clamped end, respectively. Both of these figures indicate the existence of a significant deviation in vibration amplitude at the crack initiating position when the crack depth reaches a critical value. The critical value can be defined as the ratio of crack depth to the beam section height, and has a value of 0.5, which can be useful in determining the crack size when a certain type of vibration amplitude is obtained from modal analysis in the experiments.

Further comparison of the first mode shape in Figs. 8(a) and 9(a) indicates that the mode shape of a cracked beam varies with the crack position. Notably, a distinct discontinuity appears in the deflection curve and the slope of the mode shape at the start of the crack owing to the change in the

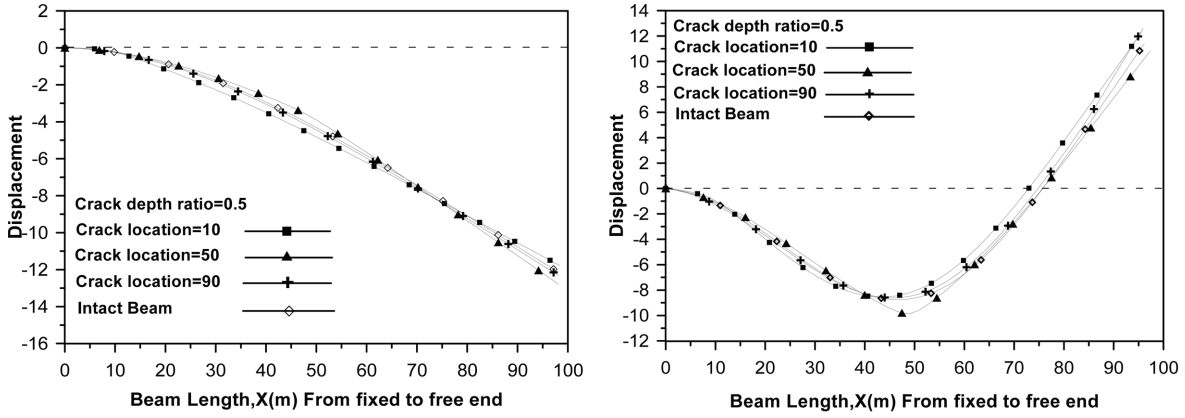

Fig. 10 Comparison of mode shape of cracked beam with a single-edge crack at different position, crack depth ratio=0.5 (a) first mode (b) second mode

structure stiffness across the crack site. As observed previously, the crack initiating position influences not only the degree of the change in nature frequency but also the mode shape. Fig. 10 shows that the mode shape of a cracked beam differs from that of the intact one. The extent of this discontinuity also depends heavily on the crack depth.

Results obtained using the current method also demonstrate that the crack location and crack depth both influence the dynamic behavior of the crack beam to different degrees. Measuring the change in natural frequencies and comparing this change to that measured for the intact beam thus can confirm the existence of a crack. For a cracked cantilever beam, the normalized natural frequency corresponding to different crack depths and crack positions can be forecast using the current method, and their relationship can be further depicted using a three-dimensional diagram, as illustrated in Fig. 11, which provides the basis for identifying crack parameters.

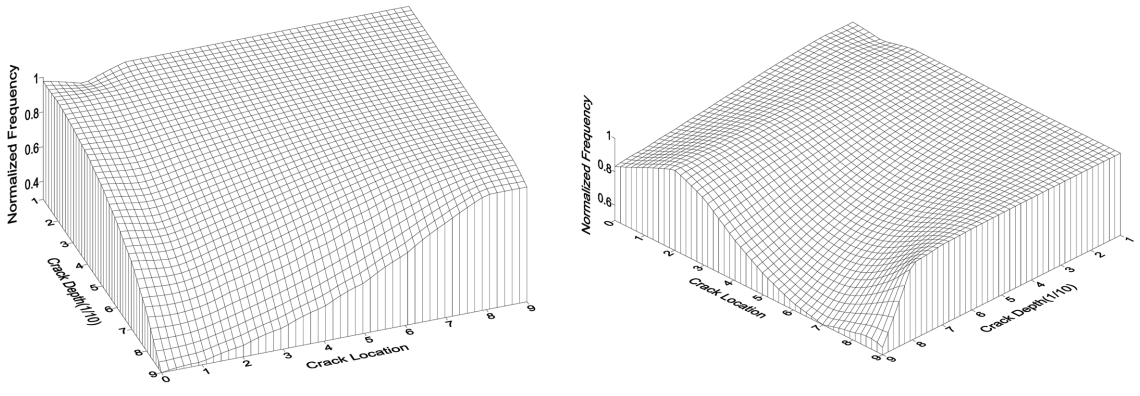

Fig. 11 Frequencies versus crack depth and crack position for a cracked cantilever beam (a) first mode (b) second mode

4. Conclusions

This study examines the dynamic behaviors of cracked structures using the finite element approach. To deal with the bilinear characteristics in cyclic vibration, a breathing crack was introduced to the cracked structures to simulate the crack in the open or closed states. The current results closely correspond to those obtained from experiments and other numerical forecasts. Although slight differences in the prediction of the vibration frequency were observed, these differences can be attributed to different considerations regarding the crack closing period of cyclic vibration. Several advantages of the proposed approach over other approaches can be summarized as follows:

1. The use of a single equivalent elastic spring element has difficulty in describing the bilinear vibration characteristics and the contact effect on the dynamic behavior. Meanwhile, a breathing crack can easily model the crack status during cyclic motion.
2. The asymmetrical motion cycle of a breathing crack was decomposed into open and closed crack periods. The bilinear natural frequency was assessed based on the overall time period of vibration. All formulae were derived in the time domain, which was different from the frequency domain.
3. The contact effect owing to mutual penetration of the crack surfaces was considered and implemented in the FE algorithm. The assumption of a fully close crack made in other studies thus was inadequate, since such a crack was not really a breathing crack. The time period of the closing crack mode can thus be estimated based on the motion path, which was shortened owing to the constrained motion.
4. The proposed method can easily be applied to other complex structures. Analytical methods generally cannot directly provide explicit results for cracked beams with different boundary conditions or crack types.

Based on the current results, we believe that the proposed method can provide a reliable and accurate means of detecting cracks initiating in other damaged structures.

References

Bovsunovsky, A.P. and Matveev, V.V. (2000), "Analytical approach to the determination of dynamic characteristics of a beam with a closing crack", *J. Sound Vib.*, **235**(3), 415-434.

Butcher, E.A. (1999), "Clearance effects on bilinear normal mode frequencies", *J. Sound Vib.*, **224**(2), 305-328.

Carson, R.L. (1974), "An experimental study of the parametric excitation of a tensioned sheet with a crack like opening", *Exp. Mech.*, **14**(2), 452-458.

Chatti, M., Rand, R. and Mukherjee, S. (1997), "Modal analysis of a cracked beam", *J. Sound Vib.*, **207**(2), 249-270.

Chen, M. and Tang, R. (1997), "Approximate method of response analysis of vibrations for cracked beams", *Appl. Math. Mech.*, **18**(3), 221-228.

Chondros, T.G. and Dimarogonas, A.D. (1980), "Identification of cracks in welded joints of complex structures", *J. Sound Vib.*, **69**(4), 531-538.

Chondros, T.G. and Dimarogonas, A.D. (1989), "Dynamic sensitivity of structure to cracks", *J. Vib., Acoustics, Stress, and Reliability in Design*, **111**, 251-256.

Chondros, T.G., Dimarogonas, A.D. and Yao, J. (1998), "A continuous cracked beam vibration theory", *J. Sound Vib.*, **215**(1), 17-34.

Chondros, T.G., Dimarogonas, A.D. and Yao, J. (2001), "Vibration of a beam with a breathing crack", *J. Sound*

Vib., **239**(1), 57-67.
Dimarogonas, A.D. (1996), "Vibration of cracked structure – A state of the art review", *Eng. Fracture Mech.*, **5**, 831-857.
Fernandez, S.J. and Navarro, C. (2002), "Fundamental frequency of cracked beams in bending vibrations: An analytical approach", *J. Sound Vib.*, **256**(1), 17-31.
Gounaris, G. and Dimarogonas, A.D. (1988), "A finite element of a cracked prismatic beam for structural analysis", *Comput. Struct.*, **28**(3), 309-313.
Gudmundson, P. (1983), "The dynamic behavior of slender structures with cross-sectional cracks", *J. Mech. Phy. Solids*, **31**(1), 329-345.
Hjelmstad, K.D. and Shin, S. (1996), "Crack identifcation in a cantilever beam from modal response", *J. Sound Vib.*, **198**(1), 527-545.
Khiem, N.T. and Lien, T.V. (2001), "A simplified method for natural frequency analysis of a multiple cracked beam", *J. Sound Vib.*, **245**(4), 737-751.
Khiem, N.T. and Lien, T.V. (2002), "The dynamic stiffness matrix method in forced vibration analysis of multiple-cracked beam", *J. Sound Vib.*, **254**(3), 541-555.
Kikidis, M.L. (1992), "Slenderness ratio effect on cracked beam", *J. Sound Vib.*, **155**(1), 1-11.
Kisa, M. (2004), "Free vibration analysis of a cantilever composite beam with multiple cracks", *J. Comp. Sci. Tech.*, **64**(9), 1391-1402.
Kisa, M. and Brandon, J. (2000), "Effects of closure of cracks on the dynamics of a cracked cantilever beam", *J. Sound Vib.*, **238**(1), 1-18.
Krawczuk, M. and Ostachowicz, W.M. (1993), "Transverse natural vibrations of a cracked beam loaded with a constant axial force", *J. Vib. and Acoustics Transactions of the ASME.*, **115**(4), 524-528.
Lee, H.P. and Ng, T.Y. (1994), "Natural frequencies and modes for the flexural vibration of a cracked beam", *J. Appl. Acoustics.*, **42**(2), 151-163.
Liew, K.M. and Wang, Q. (1998), "Application of wavelet theory for crack identification in structures", *J. Eng. Mech.*, **124**(2), 152-157.
Lin, H.P. (2004), "Direct and inverse methods on free vibration analysis of simply supported beams with a crack", *Eng. Struct.*, **26**(4), 427-436.
Murphy, K.D. and Zhang, Y. (2000), "Vibration and stability of a cracked translating beam", *J. Sound Vib.*, **237**(2), 319-335.
Nandi, A. and Neogy, S. (2002), "Modelling of a beam with a breathing edge crack and some observations for crack detection", *J. Vib. Control.*, **8**(5), 673-693.
Narkis, Y. (1994), "Identification of crack location in vibrating simply supported beams", *J. Sound Vib.*, **172**(4), 549-558.
Qian, G.L., Gu, S.N. and Jian, J.S. (1990), "The dynamics behavior and crack detection of a beam with a crack", *J. Sound Vib.*, **138**(1), 233-243.
Shen, M.H. and Pierre, C. (1990), "Natural modes of Bernoulli-Euler beams with symmetric cracks", *J. Sound Vib.*, **138**(1), 115-134.
Todd, M.D. and Virgin, L.N. (1996), "Natural frequency computations of impact oscillator", *J. Sound Vib.*, **194**(3), 452-460.
Yokoyama, T. and Chen, M.C. (1998), "Vibration analysis of edge-cracked beams using a line-spring model", *Eng. Fracture Mech.*, **59**(3), 403-409.